Electrical and Mechanical Insights of Human Atrial Fibrillation

PhD Thesis

László Sághy, MD

Second Department of Medicine and Cardiology Center
University of Szeged

Szeged,
2012

TABLE OF CONTENTS

List of Publications Related to the Thesis

List of Abbreviations

List of Figures and Tables

Summary

Introduction

Methods 1.

CFAE Maps

Sinus Rhythm Fractionation Map

Left Atrial Activation Maps During Sinus Rhythm and

Coronary Sinus Pacing

Control group

Quantitative analysis

Voltage analysis

Statistical analysis

Methods 2.

Ablation procedure

Patient follow-up

Echocardiography

Statistical analysis

Methods 3.

Electrophysiological study and follow-up

Signal analysis

Statistical analysis

Results 1.

Comparison of AF CFAE and SR Fractionation Maps

SR Fractionation and Wavefront Collision

Control group

Voltage characteristics

Results 2.

Follow-up echocardiography

Results 3.

Discussion

Conclusion

References

Acknowledgements

Összefoglalás

Appendix

Publications I-IV

LIST OF PUBLICATIONS RELATED TO THE THESIS

I Sághy L, Callans DJ, Garcia F, Lin D, Marchlinski FE, Riley M, Dixit S, Tzou WS, Haqqani HM, Pap R, Kim S, Gerstenfeld EP. Is there a relationship between complex fractionated atrial electrograms recorded during atrial fibrillation and sinus rhythm fractionation? Heart Rhythm. 2012 Feb;9(2):181-8 IF: 4.2

II. Sághy László, Vassil Borislavov Traykov, Gingl Zoltán, Pap Róbert, Forster Tamás. Frekvenciaanlízis pitvarfibrillációban. Cardiologia Hungarica 2009; 39 : 229–235 IF:-

III: Gertz ZM, Raina A, Sághy L, Zado ES, Callans DJ, Marchlinski FE, Keane MG, Silvestry FE. Evidence of atrial functional mitral regurgitation due to atrial fibrillation: reversal with arrhythmia control. J Am Coll Cardiol. 2011 Sep 27;58(14):1474-81. IF:14,2

IV: Tzou WS, Sághy L, Lin D. Termination of persistent atrial fibrillation during left atrial mapping. J Cardiovasc Electrophysiol. 2011 Oct;22(10):1171-3. IF: 3,28

SUMMARY

Introduction Atrial fibrillation (AF) is the most common supraventricular arrhythmia in humans. Arrhythmogenic thoracic veins have been implicated not only in the initiation, but also in the perpetuation of atrial fibrillation. Pulmonary vein isolation is a mainstay technique of treatment of paroxysmal AF (PAF), however, ablation of persistent atrial fibrillation may require adjunctive methods of substrate modification. Both ablation targeting complex fractionated atrial electrograms (CFAE) recorded during AF and fractionated electrograms recorded during sinus rhythm (SRF) have been described but the relationship of CFAE to SRF is unclear.

One possible way to achieve that is by measuring and averaging the cycle length (CL) of atrial activation at different sites across the atria in the time domain, however CFAEs frequently present a major obstacle to accurate CL measurement. Therefore another approach that is gaining popularity is to use spectral analysis of atrial electrograms which can be helpful when presenting spatial distribution of atrial rate in arrhythmias such as AF that show some irregularity in CL or signal amplitude.

Beyond the electrical considerations of AF, the potential mechanical consequences are also important and multiple factors contribute to functional mitral regurgitation (MR) in patients with AF. The relationship between AF associated left atrial (LA) remodeling, and its influence on the mitral apparatus have not been investigated.

Objectives

1. To elucidate the relationship between the distribution of CFAE/fragmented areas in the LA during AF and fragmented areas during SR, and analyse the mechanism of electrogram fractionation during SR.

2. To test our hypothesis that AF control after radiofrequency ablation (RFA) would result in reduction in MR by facilitating beneficial remodeling of the LA and mitral apparatus.

3. Using spectral analysis of AF, to investigate the distribution of dominant frequencies

(DFs) in the atria and pulmonary veins (PVs) during PAF and the response to arrhythmogenic PV isolation.

Methods

1. Twenty patients (age 62±9 yrs, 13 male) with persistent AF and 9 control subjects without organic heart disease or AF (age 36±6, 4 male) underwent detailed CFAE and SRF LA electroanatomic maps. The overlap in left atrial regions with CFAE and SRF were compared in the AF population, and the distribution of SRF was compared among AF patients and normal controls. Propagation maps were analyzed to identify activation patterns associated with SR fractionation.

2. We performed a retrospective cohort study. Patients undergoing first AF ablation (n: 828) were screened. Included patients had echocardiograms at the time of ablation and at 1-year clinical follow-up. The MR cohort (n: 53) had at least moderate MR. A reference cohort (n: 53) was randomly selected from those patients (n: 660) with mild or less MR. Baseline echocardiographic and clinical characteristics were compared, and the effect of restoration of sinus rhythm was assessed by follow-up echocardiograms.

3. Arrhythmogenic structures inducing PAF were identified during isoproterenol challenge in 26 patients (15 males, 55.00 ± 8.47 years). During sustained PAF sequential recordings were made with a decapolar circular mapping catheter from each PV and the left atrial posterior wall (LAPW), together with coronary sinus (CS) and right atrium (RA) recordings. DF was determined using Fast-Fourier Transformation. RFA was directed first at arrhythmogenic PVs.

Results

1. SRF (338±150 points) and CFAE (418±135 points) regions comprised 29±14 and 25±15 % of the LA surface area, respectively. There was no significant correlation between SRF and CFAE maps (r=0.2, P=NS). Comparing AF patients and controls, there was no significant difference in the distribution of SRF between groups (p=0.74).

Regions of SRF overlapped areas of wavefront collision 75±13% of the time.

2. MR patients were older than controls and more often had persistent AF (62% vs. 23%, p <0.0001). MR patients had larger left atria (volume index: 32 cm3/m2 vs. 26 cm3/m2, p =0.008) and annular size (3.49 cm vs. 3.23 cm, p = 0.001), but similar left ventricular size and ejection fraction. Annular size, age and persistent AF were independently associated with MR. On follow-up echocardiogram, patients in continuous sinus rhythm had greater reductions in left atrial size and annular dimension, and lower rates of significant MR (24% vs. 82%, p= 0.005) compared with those in whom sinus rhythm was not restored.

3. PAF initiated from the PVs in 24 patients and from RA in two. There was a significant frequency gradient from the arrhythmogenic structure to the PVs, CS, LAPW and RA (p < 0.0001). Sixty for percent of patients had AF termination upon isolating the arrhythmogenic PV antrum.

Conclusion

There is little overlap between regions of CFAE during AF and regions of SR fractionation measured in the time or frequency domain and the majority of SRF appears to occur in regions with wavefront collision. The distribution of SRF is similar in normal controls suggesting this may not have an important role in AF maintenance and may not be a suitable ablation target.

With AF control after RFA patients with significant MR at baseline, had reduction in MR, LA dimensions and mitral annular size. These observations suggest a relationship between AF induced LA remodeling, mitral annular dilatation and functional MR that can be reversed with control of AF after RFA.

Triggering structures harbor the fastest activity and consequently show the highest DF during sustained PAF pointing to their leading role in perpetuating the arrhythmia.

Introduction

Atrial fibrillation (AF) is the most common supraventricular arrhythmia in humans. For many years it has been considered a "random" process. However, research during the last decade has indisputably shown that there is a pattern of organization in this arrhythmia. The landmark discovery of Haissaguere et al. that AF is frequently initiated by ectopic beats arising from the pulmonary veins (PVs) has shed light on its initiation, and since than, pulmonary vein isolation (PVI) has become a well-established and successful method of treatment for paroxysmal atrial fibrillation (1). However, the success rate using the same strategy has been suboptimal in the persistent AF population and the mechanisms of AF maintenance are still a subject of debate.(2) Moe et al. first attempted to explain AF maintenance by the multiple wavelet hypothesis (3) that was later corroborated by the studies of Allesie et al (4). In recent years there is accumulating evidence from animal experiments and human data that AF is maintained by rotors that demonstrate regular fast activity and fibrillatory conduction to the rest of the atria producing the well known irregularly irregular ECG pattern of AF (4-6). This theory fuelled research into accurate mapping and representation of atrial rate throughout the atria during AF because sites of high atrial rate might represent structures critical to AF initiation and maintenance and amenable to ablation.

One possible way to achieve that is by measuring and averaging the cycle length (CL) of atrial activation at different sites across the atria in the time domain (7). However complex fragmented atrial electrograms (CFAE) frequently present a major obstacle to accurate CL measurement. Therefore another approach that is gaining popularity is to use spectral analysis of atrial electrograms which can be helpful when presenting spatial distribution of atrial rate in arrhythmias such as AF that show some irregularity in CL or signal amplitude.(4-6,8-11).

These observations that AF triggering and maintenance mechanisms may be different, and thus ablation of persistent AF may necessitate targeting of both triggers and substrate has led to the development of techniques for modifying the left atrial substrate in the persistent AF population.

Targeting of CFAEs recorded during AF described by Nademanee et al. as a stand-alone AF ablation procedure with a high success rate (12). However, other investigators have not been able to confirm similar efficacy (13, 14). Consequently, it has often been applied as an adjunctive technique to PVI. The mechanism(s) underlying CFAE observed during AF remain unclear. Numerous experimental and clinical studies suggest that CFAE can represent potential sources important to the perpetuation of AF,(15-19), while others have demonstrated that this phenomenon may represent passive wavefront collision. (20).

Fractionated electrograms also have been observed in the left atrium (LA) during sinus rhythm (SR) in patients with AF (21) It has been proposed by Pachon and colleagues that complex electrogram morphologies in SR recorded by frequency domain techniques and termed “AF Nests,” can serve as a pathologic substrate for AF(22). Radiofrequency ablation of these sites in SR had a favorable impact on long-term arrhythmia control in both paroxysmal and persistent AF patients in one study (23).

There is substantial evidence demonstrating a direct association between AF and LA remodelling.(24) The most important clinical hallmark of remodelling is LA dilatation. It has generally been thought that AF develops primarily as a consequence of LA dilatation, which is caused by various underlying pathologic processes, such as hypertension or coronary heart disease. However, this hypothesis does not explain the occurence of AF in patients who do not have any obvious structural heart disease; nonetheless, atrial enlargement is observed in these patients as well. (25)

Moreover, there is a linear relationship between the magnitude of LA dilatation and the duration of arrhythmia in patients with persistent AF, (25) and after succesful cardioversion or RFA, LA size may decrease and LA function improves significantly (26, 27, 28). Accordingly, it seems that AF can be a cause, as well as a consequence of the LA remodelling process (29). The association between the LA size/dilatation and mitral valve function is less well understood. The competent mitral valve needs well coordinated function of mitral annulus (MA), left ventricle (LV), and LA.(30)

Even patients with lone AF may have MA dilatation comparable to dilated cardiomyopathy (DCM) patients , (31) and it has been shown that MA enlargement play

a central role in the development of functional mitral regurgitation (MR) (32). Additionally, MA area is more closely associates with LA than LV volume indexes in a DCM population; consequently, LA size can affect mitral annular size even independent of LV dimensions, and isolated left atrial enlargement may cause mitral regurgitation in the presence of normal LV size and a structurally intact mitral apparatus. (32, 33)

Based upon the informations, mentioned above, the purposes of the present work were the following

1.: Since CFAE recorded during AF and fractionated electrograms recorded during sinus rhythm (SRF) have both been suggested as an ablation target, we sought to elucidate the relationship between the distribution of CFAE/fragmented areas in the LA during AF and fragmented areas during SR, and the mechanism of electrogram fractionation during SR.

2.: According to the observations associated with AF and LA remodelling we hypothesized that the prevalence of mild to moderate or more severe MR is higher in the population of patients candidate for RFA of AF and after a succesful procedure the functional MR may decrease as a consequence of reverse LA and mitral annular remodelling.

3.: In order to provide reliable electrical information about the arrhytmogenic structures that are responsible for the genesis of atrial fibrillation we performed initial methodological testing of spectral analysis.

Methods 1.

Patients undergoing ablation of persistent AF were included in the study. Persistent AF was defined as AF that persisted > 1 month or that typically required cardioversion for AF termination. All patients provided written informed consent. Antiarrhythmic medications were held more than five half lives before the procedure, except amiodarone which was held for 1 week.

Decapolar catheters were placed in the posterior right atrium (RA) and coronary sinus. A circular mapping catheter (10-pole, adjustable 15–25-mm Lasso, 6-mm bipole spacing,

Biosense Webster, Diamond Bar, CA, USA) and a 3.5-mm tip irrigated ablation catheter (Celcius Thermocool, Biosense Webster; Diamond Bar CA) were introduced in the LA through double transseptal puncture. IV heparin was infused throughout the procedure to maintain an ACT of >350 seconds.

CFAE maps

A three-dimensional LA geometry was created using the NavX electroanatomic mapping system (NavX, St. Jude Medical, St. Paul, MN). After the geometry was created, a detailed bipolar LA CFAE map was acquired during AF using the circular mapping catheter; undersampled areas were filled in using the ablation catheter (<10% of all points). The CFAE map was acquired on-line using automated NavX algorithm. At each point, deflections above baseline were automatically detected, and the mean AF fractionation interval (FI) was calculated by averaging the intervals between deflections over a 5-second window. (refractory period = 50 ms; width =10ms; sensitivity 0.05 – 0.1mV). The sensitivity was adjusted on a per patient basis. The lasso catheter was placed distally into a pulmonary vein where no atrial musculature was present, and the detection sensitivity was set just above the level of background noise. Points were only included if they were within 8 mm of the geometry shell, thus minimizing the acquisition of internal or external points that were not in contact with the LA. Regions with a mean FI < 70ms were defined as the CFAE. After the procedure, all points were manually over-read and signals with significant noise were excluded. All intracardiac signals were acquired at a sampling frequency of 1200 Hz.

Sinus Rhythm Fractionation Map

After DC cardioversion to sinus rhythm followed by a 5-minute waiting period, a second detailed bipolar LA activation map was acquired in SR, using the same circular mapping catheter. Care was taken to assure an even distribution of points throughout the left atrial geometry. Offline, premature atrial beats were eliminated. Sinus rhythm fractionation (SRF) was calculated manually for each electrogram by counting the number of deflections present in each electrogram (Figure 1) and recoding the total number of deflections as the peak-to-peak voltage. In this manner, a color-coded sinus

rhythm “fractionation map” could be displayed. (Figure 2).

Normal conduction typically results in three deflections of the bipolar electrogram (34). In order to determine a cutoff for the number of deflections that was considered “abnormal,” we determined the 95th percentile of electrogram deflections from our nine patient normal controls, after excluding septal points which have both right and left atrial components. We found that 95% of bipolar electrograms showed ≤ 5 deflections in our healthy control population, therefore electrograms with more than five deflections were defined as abnormally fragmented.

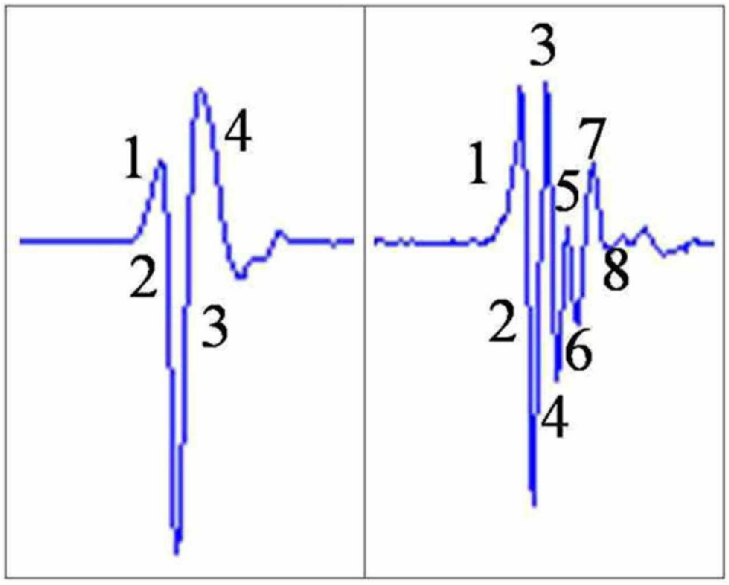

Figure 1.

Example of manual calculation of number of deflections assigned to each atrial electrogram. Each change in slope was incremented to give a total number of deflections. The atrial electrogram on the left is normal appearing and has a fractionation index of 4. The electrogram on the right is fractionated and has a fractionation index of 8.

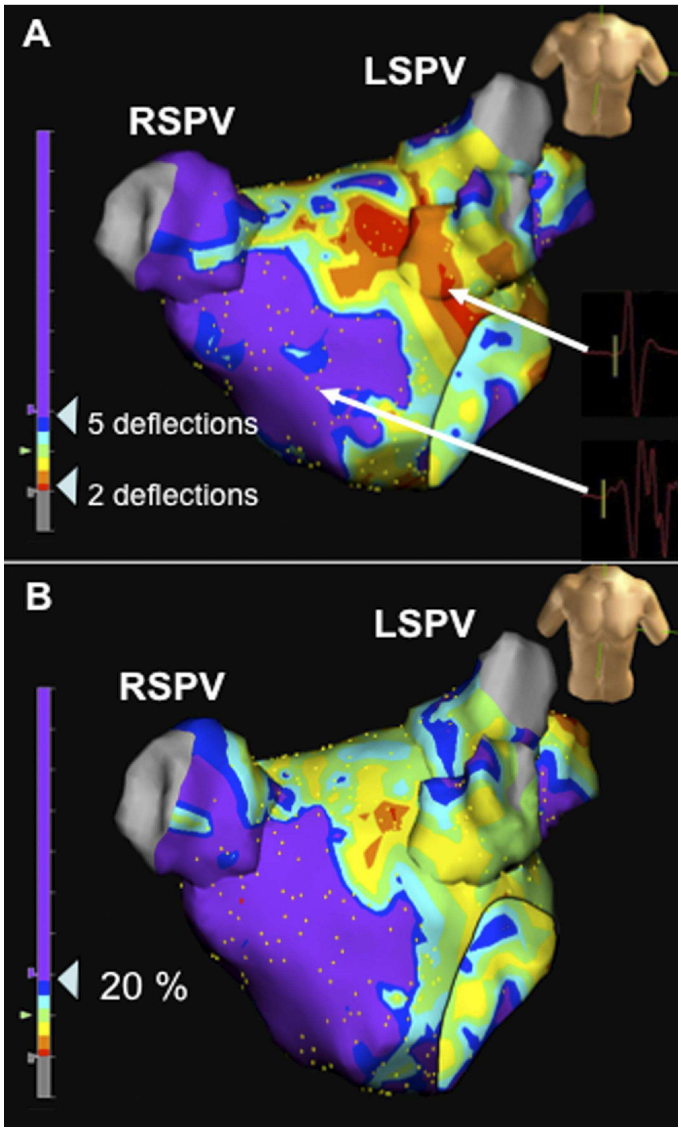

Figure 2.

A: Time domain manual LA sinus rhythm fractionation map in antero-posterior view using NavX 3 D mapping system. The number of deflections was manually counted for each electrogram and displayed on the left atrial map (>5 deflections=purple). A representative electrogram from a fractionated and a non fractionated region is shown on the right. B: Automated FFT ratio map (FFT ratio >20%=purple). Note the similarity in the appearance of the two maps. FFT = Fast Fourier Transformation; LSPV = left superior pulmonary vein; RSPV = right superior pulmonary vein.

A frequency domain measure of left atrial sinus rhythm bipolar electrogram fractionation was also used. The "FFT ratio" (Fast Fourier Transformation ratio, FFTr) of high(>100 Hz) to total (0-300 Hz) spectral power was automatically computed and displayed on the electroanatomic map using a customized version of the NavX software (Figure 3). We found that an FFT ratio cutoff of >20% identified areas of fractionated electrograms during sinus rhythm.

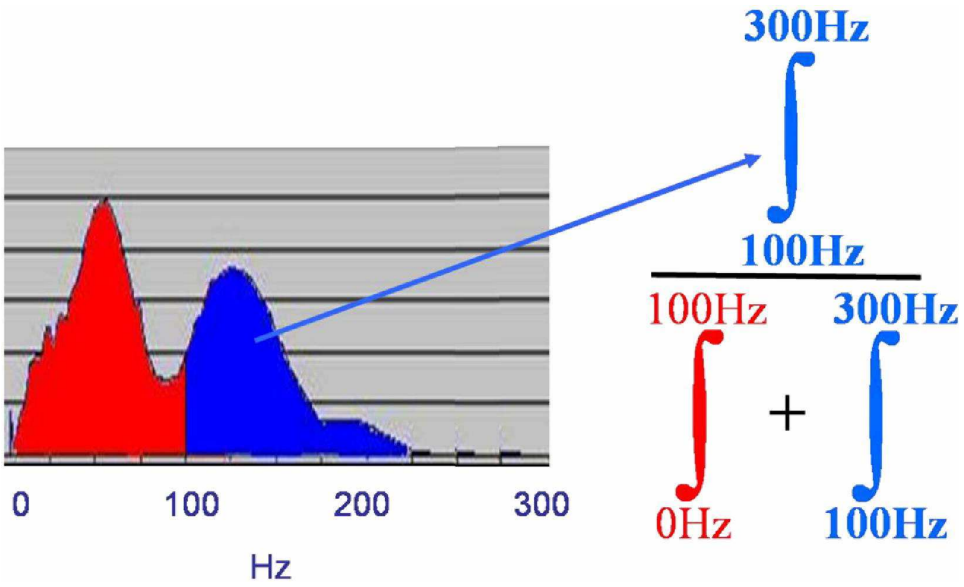

Figure 3.

Calculation of FFT ratio. The frequency spectrum of the sinus rhythm atrial electrogram is first calculated by taking applying a Hanning window and then calculating a 1024 point FFT. The area under the curve from 100-300Hz is then divided by the area under the entire spectrum to calculate the FFT ratio. This ratio is higher for fractionated electrograms. FFT: Fast Fourier Transfromation

Left Atrial Activation Maps During Sinus Rhythm and Coronary Sinus Pacing

The high density sinus rhythm maps also allowed a detailed reconstruction of left atrial endocardial activaton. Regions of SRF were outlined on the LA geometry and activation patterns in regions of SR fractionation were examined in order to determine the mechanisms of fractionation. We hypothesized that areas of sinus rhythm fractionation

might be related to wavefront collision, and therefore areas of wavefront collision were all manually annotated on the maps.

Finally, we also altered the pattern of wavefront propagation by pacing from the distal coronary sinus and repeating a third detailed bipolar activation map during coronary sinus pacing. The overlap between regions of LA fractionation recorded during CS pacing and regions of wavefront collision during CS pacing was calculated.

Control group

In order to determine the distribution of SRF in normal controls, nine control subjects without structural heart disease or history of AF underwent detailed bipolar LA maps in SR (CARTO XP, Biosense Webster, Diamond Bar, CA). These patients had all undergone mapping and ablation of paroxysmal supraventricular tachycardia (3 Wolf-Parkinson-White syndrome, 4 concealed left lateral accessory pathways, 1 focal atrial tachycardia).

Quantitative analysis

The LA surface was divided into 9 segments: left pulmonary veins, right pulmonary veins, roof, septum, anterior wall, lateral wall, posterior wall, left atrial appendage and mitral annulus (extending 1 cm from the mitral valve plane). Each AF CFAE region, each SR fractionation region and each CS pacing fractionated region was outlined. The percentage of each anatomic segment that was encompassed by each fractionated region was calculated for each map. The percent overlap between CFAE and SRF was counted as the area common to both CFAE and SRF divided by the total area of CFAE. (Figure 4). CFAE and SRF data were also exported to SPSS to calculate a correlation coefficient between maps. Since the total number and location of CFAE and SRF points differed for each map, we exported the 1024 evenly spaced map data points that were calculated by the NavX system using linear interpolation.

The percent overlap between the fractionated areas on the manual and automated FFtr maps was calculated as the area common to both regions divided by the total area of SRF in each segment. The percentage of areas of wavefront collision that were within regions of fractionation (# collisions within fractionated area / total # collisions) was calculated

for the sinus rhythm and CS pacing maps.

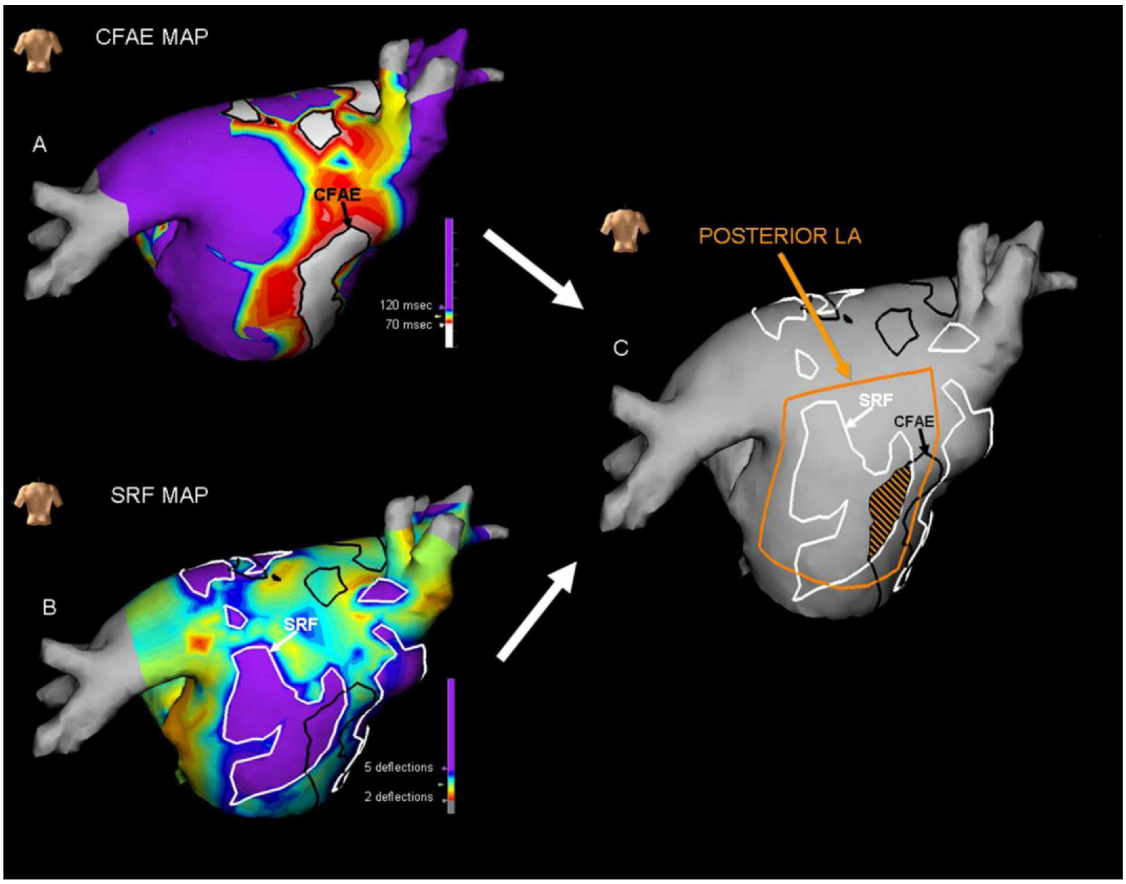

Figure 4

Left atrial CFAE map acquired during atrial fibrillation using NAvX 3D mapping system (panel A). White colour represents CFAE areas, outlined with black. Left atrial manual sinus rhythm fragmentation map in the same patient and same view (panel B). Purple colour represents the fragmented areas in sinus rhythm, outlined with white. Panel C demonstrates the calculation method of overlap between the left atrial CFAE and sinus rhythm fragmentation areas (brown striped area). CFAE: Complex fractionated electrograms, SRF: sinus rhythm fragmentation, LA: left atrium

Voltage analysis

Since the voltage characteristics of normal human LA are not well defined, we measured the global and regional unipolar (UNI) and bipolar (BI) signal amplitudes in

the control patients to determine the optimal voltage cutoff for the normal left atrium. These data served as a standard for comparing the regional distribution of low voltage areas in AF population and controls. Finally, we analyzed the voltage in regions of SRF in AF patients compared to healthy controls. For the unipolar voltage analysis in healthy controls we used Wilson's central terminal as a reference pole. Unipolar signals were filtered from 0.05Hz -500 Hz, and bipolar signals from 30 -500 Hz.

Statistical analysis

Data are presented as mean ± 1 standard deviation. Continuous data were compared by using Student's t test and categorical data with the χ^2 test. For the map comparisons, a Pearson's correlation coefficient was calculated between the SRF and CFAE maps and linear regression was used to calculate statistical significance. Comparison of the proportion of fractionated SR electrograms and low-voltage areas in each region between the control and AF patients was performed by using multivariate analysis of variance. A *P* value of <.05 was considered significant.

Methods 2.

We performed a retrospective cohort study to determine whether AF is associated with significant atrial functional MR.

The institutional review board at the University of Pennsylvania approved the study. All patients referred to the University of Pennsylvania Health System for catheter ablation of drug refractory AF between June 2003 and December 2008 were eligible for inclusion. Reports from transthoracic echocardiograms performed within 3 days of catheter ablation of AF were screened, and an experienced research echocardiographer analyzed the images of those with greater than mild MR. All patients with secondary Type I MR of at least moderate severity (as described in the following text) and who also had complete 1-year clinical follow-up after ablation were included in the MR cohort. The reference cohort was randomly selected in a 1-to-1 fashion from those patients with mild or less MR on initial report screening and subsequent image analysis and who also had complete

1-year clinical follow-up. Patients with an ejection fraction <50% were excluded to avoid including patients whose MR might be due to ventricular dysfunction. Demographic and clinical information were prospectively obtained in all patients. The clinical AF syndrome was determined based on the predominant arrhythmia presentation at the time of admission and was defined as paroxysmal if AF episodes were self-terminating in < 7 days and persistent if typical AF episodes lasted >7 days and/or required intervention for termination.

Ablation procedure

All patients underwent proximal antral PVI, guided by intracardiac echocardiogram and circular multipolar electrode catheter recordings and elimination of all provocable PV triggers and all non-PV triggers resulting in AF, as previously described (Methods 1). All 4 PVs were isolated routinely in patients with a history of persistent AF, those without provocable AF triggers, and those patients with significant risk factors for AF including a history of hypertension, LA enlargement, and those over the age of 50 years. In the remaining selected patients, we isolated arrhythmogenic PVs only.

Patient follow-up

Patients were routinely treated with previously ineffective antiarrhythmic medications (usually a class 1C agent or sotalol) prior to discharge. The patients were clinically evaluated as outpatients at 6 to 12 weeks, 6 months, and 1 year, at which time they were queried for symptoms and 12-lead electrocardiograms were obtained. Echocardiograms were performed at the first visit and at the second or third visits, at the treating physician's discretion. Antiarrhythmic medications were typically discontinued at 6 to 12 weeks if patients had paroxysmal AF and at 6 months if they had persistent AF, but were continued beyond this point in selected patients based on doctor and/or patient preference even in the absence of an arrhythmia event. The patients were provided with a transtelephonic monitor (TTM) and instructed to transmit 2 times daily and with symptoms during the first 4 weeks after ablation. They were then instructed to transmit

once at 6 to 12 weeks, then once at 6 months and 1 year. Patients also made additional TTM transmission if they had any arrhythmia symptoms at any time during follow-up and/or when antiarrhythmic medications were discontinued. Source documentation of arrhythmia recurrence was sought. The first 3 months after ablation were censored from follow-up for judging recurrence. One-year AF recurrence was defined according to consensus guidelines as any documented electrocardiographic episode of atrial arrhythmia lasting 30 s or longer with or without symptoms (35). Recurrence at the time of follow-up echocardiography was defined as any electrocardiographic recurrence during the 6 months preceding the echocardiogram.

Echocardiography

Standard 2-dimensional and Doppler echocardiography with color flow mapping was performed according to the standard clinical protocol at the University of Pennsylvania Health System. Echocardiograms were then analyzed offline using digital analysis software (KinetDx, Siemens, Mountain View, California) by a single research echocardiographer, blinded to patient outcomes and to the relative timing of the echocardiogram. LA anterior–posterior systolic diameter was measured in the parasternal long-axis view, and the major axis of the LA was measured in the apical 4-chamber view. LA area at endsystole was measured in the apical 2- and 4-chamber views. Similarly, LA volumes at end-systole were measured in the apical 2- and 4-chamber views using a single-plane modified Simpson's method of discs, and values averaged. Mitral annular dimensions were measured in parasternal long-axis, apical 2-chamber, and apical long-axis views. MR color jet area was measured in the apical 4-chamber, apical 2-chamber, and apical long-axis views. Color Doppler scale and, therefore, Nyquist limit were determined by the clinical ultrasonographer and in general were set to 50 to 70 cm/s. The ratio of MR color jet area to LA area (MR/LA ratio) was then calculated, using the largest measured values for both. Mild MR was defined as a MR/LA ratio of $\geq$0.1 to $\leq$0.2, moderate MR as $\geq$0.2 to $\leq$0.4, and severe as $\geq$0.4. Only patients with moderate or greater MR were included in the MR cohort. Leaflet

motion was characterized as normal, excessive, or restrictive Only patients with normal mitral leaflet motion (Carpentier Type I) were included in the MR cohort. Patients with any evidence of primary leaflet involvement, such as from prior endocarditis, rheumatic valve disease, congenital anomaly, or significant mitral annular calcification, were excluded.

Statistical analysis

This study had 2 primary analyses. The first was to define the clinical and echocardiographic characteristics associated with significant atrial functional MR. The second primary analysis was the change in MR severity associated with restoration of sinus rhythm. All continuous variables are presented as mean ± SD, categorical values are presented as percentages, and odds ratios are presented with 95% confidence intervals (CIs). For comparisons between the MR and reference cohorts, continuous variables were compared with a *t* test, and categorical values were compared using a chi-square test. For paired samples within groups, continuous variables were compared using a paired *t* test. We performed binary logistic regression in order to detect the variables that were independently associated with significant MR. All models were constructed using those variables whose univariate correlation with significant MR had $p \leq 0.1$. For the between-group comparisons of MR grade by category, we used a Wilcoxon rank sum test. All significance tests were 2-tailed, and $p < 0.05$ was considered significant.

Methods 3.

To test the spectral analysis of AF we aimed to characterize the dominant frequency (DF) distribution in the atria and PVs shortly after initiation and during sustained paroxysmal AF in relation to the specific arrhythmogenic structure triggering the episode.Test patients were included if they had frequent episodes of PAF resistant to at least one antiarrhythmic medication. PAF was defined according to the currently accepted criteria. Exclusion criteria were previous catheter ablation for PAF, non-paroxysmal AF, previous heart surgery involving atriotomy, severe valvular heart disease, LA thrombosis and/or

contraindications to prolonged anticoagulation.. Antiarrhythmic medications were withheld for at least 5 half-lives apart from amiodarone which was discontinued 1 month before the procedure.

Electrophysiological study and follow-up

After written informed consent was obtained all patients were studied in the fasting state under light conscious sedation with midazolam±fentanyl. Following femoral venous access decapolar steerable electrophysiologic catheters (interelectrode spacing 2-5-2 mm, Dynamic Deca, Bard Electrophysiology, Lowell, MA, USA) were positioned in the CS and at the posterolateral RA wall with the distal bipole at the junction between the RA and superior vena cava (SVC). After double transseptal puncture a decapolar circular mapping catheter (Inquiry Optima, St. Jude Medical, Irvine, CA, USA) and a quadripolar, 3,5 mm irrigated tip mapping/ablation catheter (Navistar Thermocool, Biosense Webster, California, USA) were advanced to the LA. Intracardiac echocardiography (ICE) (AcuNav, Acuson Corp, Mountain View, CA, USA) was used to define the PV ostia and to guide catheter positioning. Initially, the circular mapping catheter was positioned at the left PV antrum and the mapping/ablation catheter was steered to the carina between the right PVs (Figure 5). If the patient presented to the EP lab in sinus rhythm PAF induction was attempted by isoproterenol infusion at a starting dose of 3 μg/min with subsequent increments of 5 μg/min until PAF was induced, the patient developed side effects or the maximum dose of 20 μg/min was reached.

If the presenting rhythm was AF transthoracic electrical cardioversion was performed before proceeding to AF induction. Atrial premature depolarizations (APDs) identified as PAF triggers were recorded using the above mentioned catheter configuration and the endocardial activation sequence was analyzed. Early activation at the poles positioned in the superior or inferior regions of the left antrum with LA-PV electrogram reversal was considered to signify left superior (LSPV) or left inferior pulmonary vein (LIPV) origin of the APDs, respectively.to determine their origin.

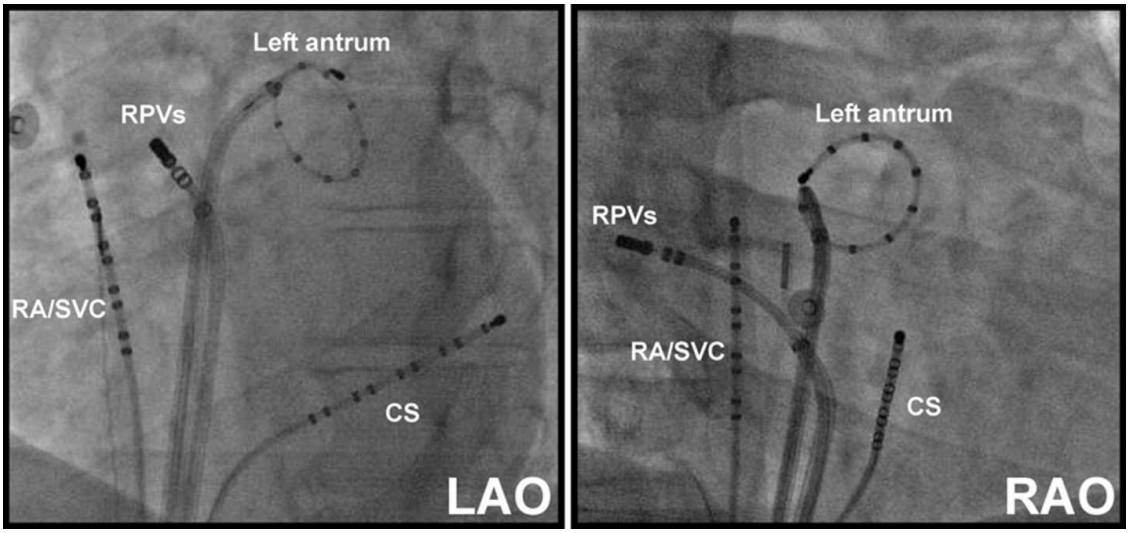

Figure 5.

Fluoroscopic views (left anterior oblique (LAO 45º) and right anterior oblique (RAO 25º) showing catheters positioned in the left PV antrum, the carina between the right PVs (RPVs), coronary sinus (CS) and the right atrium with its distal bipole in the superior vena cava (RA/SVC). This catheter configuration was used to record intracardiac signals during AF induction.

Triggers demonstrating early activation at the poles located at the level of the left carina were considered to arise from the left PVs without further specifying their origin to the LSPV or LIPV. APDs were considered to arise from the right PVs if the earliest activation during APD was recorded at the right PV carina and the quadripolar catheter positioned there demonstrated distal to proximal activation and/or LA-PV potential reversal. When earliest atrial activation was recorded at any of the CS or RA bipoles these structures were identified as triggers. Upon induction of sustained AF isoproterenol infusion was discontinued and further signal recordings were made after a 5 min waiting period. During sustained AF the circular catheter was used to record signals sequentially from each PV ostium and the LA posterior wall (LAPW) simultaneously with recordings from the RA and CS. After achieving stable catheter position as assessed by fluoroscopy and ICE, signals were recorded for at least 30 sec from all catheter bipoles at a sampling rate of 997 Hz/sec using a commercially available digital EP recording system (GE Cardiolab, General Electrics, Milwaukee, WI, USA).

Signal analysis

Intracardiac signals were analysed utilizing a custom designed computer application prepared with the LabView software package (National Instruments, Austin, Texas). Signals were bandpass filtered between 30 and 500 Hz, rectified and then low-pass filtered at 20 Hz. Following this preprocessing a FFT with a Hanning window was performed on two consecutive 5-seconds episodes of the signal from each bipole from all catheters (frequency resolution 0.2 Hz). The frequency spectrum in the 3-15 Hz range was obtained and the DF was determined as the peak with the highest power. Regularity index (RI) was also calculated as the ratio of the area under the DF peak and its harmonics to the area under the whole spectrum curve in the above mentioned frequency range The maximum DF value from all bipoles of each structure was taken as the DF of that structure and used for further analysis All recordings demonstrating RI<0.25, low signal-to-noise ratio or far-field ventricular signal with high amplitude were excluded from the analysis. Signals were also excluded if there were major discrepancies in the median AF cycle length measured manually in the time-domain.

Statistical analysis

Continuous data are presented as mean ± standard deviation (SD). The regional differences in DF distribution were analysed with one-way ANOVA. Pairwise post-hoc comparison was done after Bonferroni correction.

Results 1

Twenty patients with persistent AF were included in the study.Baseline characteristics of the patients are summarized in Table 1. Prior to ablation, patients had tried a mean of 1.4 ± 1.3 antiarrhythmic agents. One patient was taking amiodarone, and it was discontinued one week before the procedure.

Table 1. Baseline characteristics

Variables	AF patients N=20	Control subjects N=8	P
Age (years)	61 ± 9	36±6	<0.0001
Gender (% male)	75	50	0.371
*Left atrial size (cm)	4.4 ± 0.5	3.8±0.2	0.006
LVEF (%)	58 ± 9	67.8±6.5	0.020
Hypertension (%)	40	28.6	0.662
SR map points	338±150	169±37	0.002

SR: Sinus rhythm, LVEF: leftventricular ejection fraction, *: Left atrial antero-posterior diameter, measured in parasternal long axis view

Comparison of AF CFAE and SR Fractionation Maps

An average of 418 ± 135, and 338 ± 150 points were acquired for the CFAE and SRF maps, respectively. CFAE comprised 25 ±15% of the LA surface area. CFAE regions were most prevalent on the LA septum (37%), anterior wall (44%) the roof of LA (45%), and least prevalent in the LAA (14 %). SR fractionation encompassed 29 ±14% of the left atrium. SR fractionation was most prevalent on the LA septum (53%) and anterior wall (45 %), and least prevalent in the LAA (12%).

Despite the similar general distributions of the two different measures of electrogram fractionation, the location of the actual SRF and CFAE regions were typically different, with only 32±16% overlap (Figure 4). There was also no significant correlation between SR fractionation and CFAE maps (r=0.2 p= 0.24). In order to examine the influence of different settings on the overlap of CFAE and SRF, measurements were repeated with a refractory period set to 30 msec in five patients, yielding no statistical difference.

On the other hand, the appearance of the manual SR fractionation and automated FFTr maps was quite similar, with abnormal electrograms using both techniques comprising 29±14 and 31±12 % of the LA surface area, respectively. There was a significant correlation between SRF, and FFTr maps (r=0.6 p<0.01) with 75 % overlap between the

SRF and FFTr maps.

SR Fractionation and Wavefront Collision

Analyzing the left atrial endocardial activaton using the high density sinus rhythm maps, areas of wavefront collision were encompassed by regions of SRF 75±13% of the time. (Figure 6). When activation maps were then repeated during coronary sinus pacing at 500ms, there was a shift in the areas of wavefront collision. Along with these shifts in areas of wavefront collision during CS pacing, there was a parallel shift in regions of electrogram fractionation such that there continued to be an 87± 13 % overlap between areas of fractionation during CS pacing and regions of wavefront collision (Figure 7). This suggests that the majority of the regions of sinus rhythm fractionation, whether recorded during sinus rhythm or CS pacing, were due to wavefront collision rather than some inherent characteristic of the local atrial tissue.

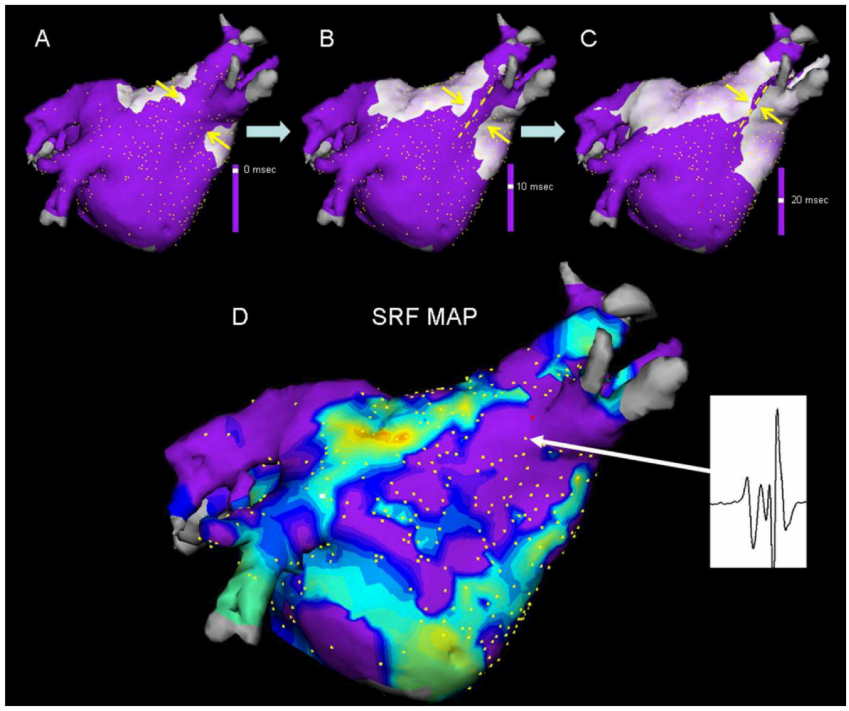

Figure 6.

Left atrial propagation map during sinus rhythm (A to C, posteroanterior view) in an AF patient. The yellow arrows depict the direction of wavefront propagation Image D shows

the left atrial sinus rhythm fragmentation map. Purple color represents the fragmented region on the posterior wall (more than 5 deflections). Fragmented electrogram is recorded (inset) where activation wavefronts collide.

SRF: sinus rhythm fragmentation

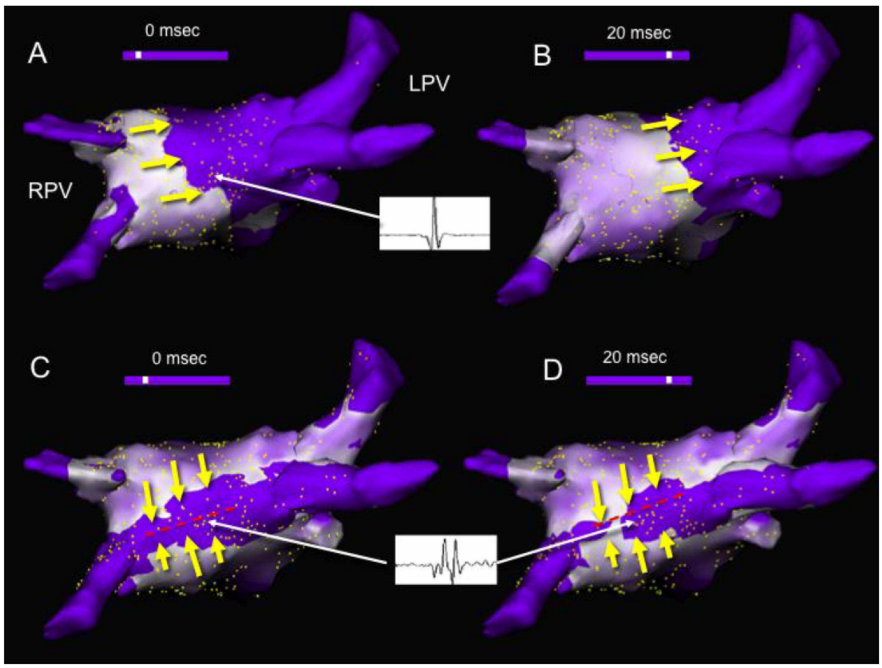

Figure 7.

Left atrial propagation map during sinus rhythm (A&B) and coronary sinus pacing (C&D) in an AF patient (NavX 3D mapping system). Craniocaudal view. White color represents depolarized myocardium. Simple, non-fragmented electrogram is recorded during sinus rhythm, where depolarization wavefront is single and homogeneous on the roof. During coronary sinus pacing, a fragmented electrogram is recorded from the same area of the roof, where opposite wavefronts collide(red broken line) RPV: right pulmonary veins, LPV: left pulmonary veins

Control group

In 9 patients with structurally normal hearts, detailed SRF maps were acquired. In normal atria, SRF was most prevalent on the LA septum (65%) and anterior wall (49%), and least prevalent in the LA appendage (8%). SRF in patients with AF and controls comprised 29±14% and 32±20% of the LA surface area, respectively. There was no

significant difference in the distribution of SRF between the 9 healthy control patients and the 20 patients with a history of AF(p=0.74, Figure 8).

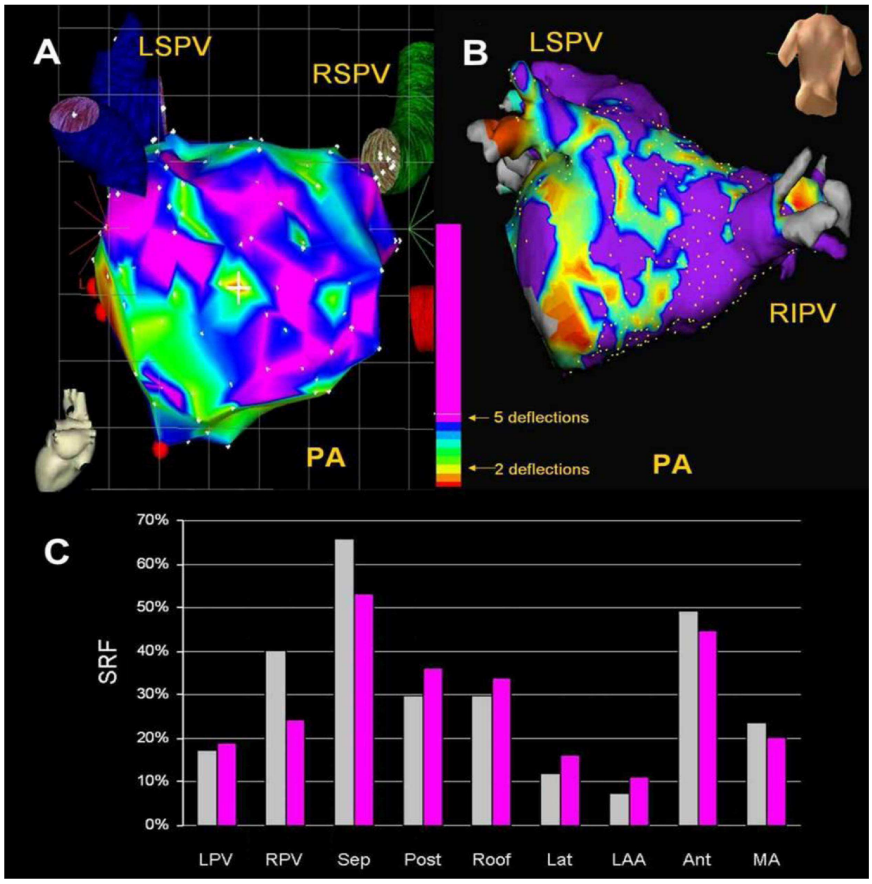

Figure 8.

SRF areas in a control patient (A), and in an AF patient (B) on the posterior wall using Carto XP, and NavX 3D mapping systems, respectively. Purple color represents the fragmented regions. Note the similarity in the appearance of the two maps. Overall distribution of SRF in controls (light grey) and AF patients (purple) (C). LSPV: left superior pulmonary vein, RSPV: right superior pulmonary vein, RIPV: right inferior pulmonary vein, LPV: left pulmonary veins, RPV: right pulmonary veins, Sep: septum, Post: posterior wall, Lat: Lateral wall, LAA: Left atrial appendage, Ant: anterior wall, MA: mitral annulus PA: posteroanterior view.

Voltage characteristics

In control patients, the global mean LA BI and UNI voltage amplitude in SR were 2.83±2.25 mV and 4.12±2.14 mV, respectively; 95% of all BI and UNI electrograms

recorded from the LA were >0.50 and >1.57 mV, respectively.

There was no difference in mean LA BI voltage between the AF patients and the controls (2.80 ± 2.75 mV vs 2.83 ± 2.25 mV; p= 0.68). Using the 0.5 mV as a BI voltage cutoff indicating abnormal atrial substrate, we calculated the percentage of low voltage areas (<0.5 mV) in each LA segment (excluding the pulmonary veins) in AF patients and normal subjects. In healthy controls, low voltage signals were present rarely in the LA septum (1%), roof (2%), anterior wall (2%), posterior wall (3%), lateral wall (4%), mitral annulus (4%), and LA appendage (0%). There was no difference in the segmental distribution of low voltage areas between AF patients and healthy controls (p=0.829).

The mean bipolar and unipolar voltage amplitude of the SRF signals (>5 deflections) were significantly lower than the non-SRF signals (bipolar 2.43±1.65 vs 3.62±2.72 mV, unipolar 4.01±1.99 vs.5.07±2.47 p < 0.0001.

Results 2

There were 97 patients who met our criteria for significant MR after study review. Of these, 54 had normal leaflet motion with no apparent primary leaflet pathology (6.5% of all patients undergoing first ablation), 53 of whom had 1-year clinical follow-up and were included as the MR cohort. One patient required mitral valve surgery in the first year after ablation, but after her 6-month echocardiogram, and was included in the analyses. Of the 660 patients with mild or less MR and 1-year clinical follow-up, 53 patients were randomly selected as the reference cohort.

Clinical characteristics of the MR and reference cohorts are shown in Table 2. Patients with MR were older, more likely to have persistent AF, and more frequently had hypertension. Ninety-seven percent of patients were in sinus rhythm at the time of their baseline echocardiogram. Echocardiographic characteristics of the MR and reference cohorts are shown in Table 3. Patients with MR had significantly larger LA size by several measures and larger mitral annular dimensions, but no difference in any measure of left ventricular size or function. Among the reference cohort, 60% had trace or no MR

and 40% had mild MR. In the MR cohort, 72% had moderate MR and 28% had severe MR.

Table 2. Clinical Characteristics of the MR and Reference Cohorts

	MR Cohort (n = 53)	Reference Cohort (n = 53)	p Value
Age, yrs	61.6 ± 8.4	55.4 ± 12.4	0.003
Male	70% (37)	66% (35)	0.68
Hypertension	62% (33)	43% (23)	0.052
Diabetes	6% (3)	11% (6)	0.30
Prior stroke or TIA	6% (3)	2% (1)	0.31
CHADS-2 score	0.9 ± 0.7	0.6 ± 0.7	0.052
Persistent AF	62% (33)	23% (12)	<0.0001

Table 3. Echocardiographic Characteristics of the MR and Reference Cohorts

	MR Cohort (n = 53)	Reference Cohort (n = 53)	p Value
LA dimension, cm	4.38 ± 0.56	4.03 ± 0.52	0.001
LAA, cm^2	21.8 ± 5.2	19.2 ± 3.3	0.003
LA volume, cm^3	68.5 ± 29.3	55.2 ± 14.1	0.004
LA volume index, cm^3/m^2	31.8 ± 12.9	26.4 ± 6.6	0.008
Mitral annulus dimension, cm	3.49 ± 0.31	3.23 ± 0.42	0.001
MRJA, cm^2	6.0 ± 2.7	1.2 ± 0.7	<0.0001
MRJA/LAA ratio	0.35 ± 0.11	0.09 ± 0.04	<0.0001
Ejection fraction, %	61.5 ± 7.1	62.2 ± 7.1	0.63
LV end-diastolic dimension, cm	5.01 ± 0.57	4.92 ± 0.49	0.39
LV end-systolic dimension, cm	3.41 ± 0.58	3.25 ± 0.62	0.17
Septal thickness, cm	1.14 ± 0.21	1.09 ± 0.19	0.21
Posterior wall thickness, cm	1.10 ± 0.17	1.06 ± 0.17	0.31

Values are mean ± SD or % (n). TIA = transient ischemic attack. LAA: left atrium area, LV = left ventricle, MRJA = mitral regurgitation jet area.

Binary logistic regression models were constructed to determine the variables that were independently associated with significant MR. Mitral annular dimension had the largest odds ratio in the final model (8.39 per cm, 95% CI: 1.94 to 36.35 per cm, p = 0.004).(Fig.9)

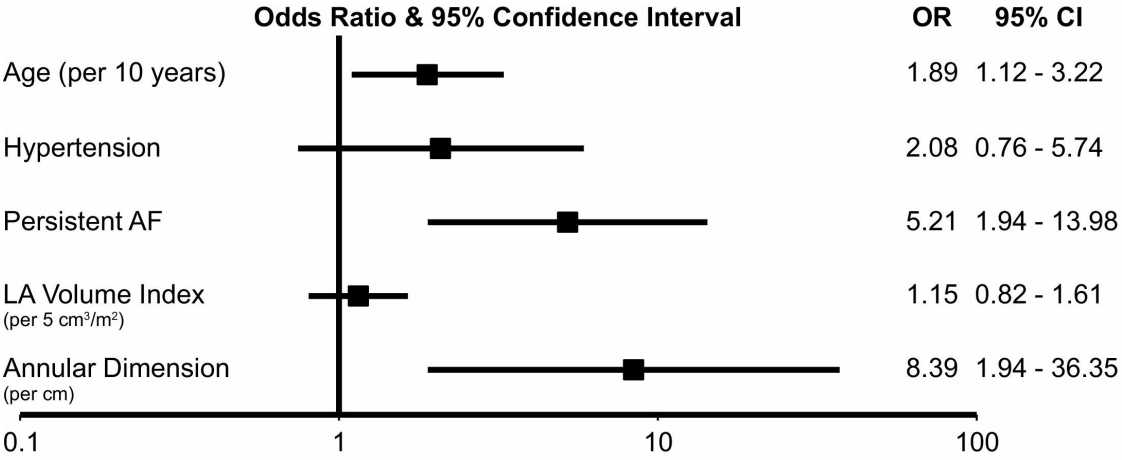

Figure 9

Forest Plot Illustrating the Independent Predictors of Atrial Functional MR. All univariate predictors with $p \leq 0.1$ were included in the model. The x-axis is on a logarithmic scale. CI = confidence interval; LA = left atrium; OR = odds ratio

Follow-up echocardiography

Follow-up echocardiograms were available in 32 of the 53 patients in the MR cohort, an average of 277 days after ablation. There were no statistically significant differences in any clinical or echocardiographic characteristics between the patients with and without follow-up echocardiograms, nor was there a difference in 1-year clinical outcome. Rhythm status at follow-up was defined as described above, applied only to the 6 months preceding echocardiography. By this definition, 21 patients were free of recurrence and 11 patients had recurrence of AF. Ninety-four percent of patients were in sinus rhythm at the time of follow-up echocardiography. At the time of ablation, patients with eventual recurrence had larger measures of LA size (LA volume index: 41.3 cm^3/m^2 vs. 28.2 cm^3/m^2, p = 0.02), with nonsignificant trends towards larger regurgitant jet area and

mitral annular dimension (Table 4). Other echocardiographic measures were not significantly different between the 2 groups at baseline.

At follow-up, both groups had reductions in LA size, but only the group in sinus rhythm had a significant decrease in mitral annular dimension (3.41 cm at baseline to 3.24 cm at follow-up, p = 0.02). Both groups experienced some decrease in MR, but at follow-up, the patients in sinus rhythm had significantly less MR than patients with AF recurrence (MR/LA ratio: 0.16 vs. 0.28, p = 0.005) (Table 4), despite being similar at baseline. Measures of left ventricular size and function remained similar between both groups at follow-up.

At baseline both groups had similar percentages of patients with moderate and severe MR (p = 0.72) (Fig.10). At follow-up, 19% of the patients in sinus rhythm had trace or no MR, compared with 0% in the recurrence group, and 57% in the sinus rhythm group had mild MR compared with 18% in the recurrence group. Only 24% of the sinus rhythm patients still had significant MR at follow-up, compared with 82% in the recurrence group (p = 0.005 for entire trend) (Fig.10).

Follow-up echocardiograms were available in 32 of the 53 patients in the reference cohort, an average 300 days after ablation. There were no statistically significant differences in any clinical or echocardiographic characteristics between the patients with and without follow-up echocardiograms, nor was there a difference in 1-year clinical outcome. Using the definition of rhythm status described above, 17 patients were in sinus rhythm and 15 had a recurrence at the time of echocardiography. There were no significant echocardiographic differences between the groups at baseline .

Table 4 Follow-Up Echocardiographic Characteristics of MR Cohort Patients With Recurrence Versus Sinus Rhythm

	Rhythm at Follow-Up Echocardiogram (Recurrence n=11, Sinus n=21)*	Initial	Follow-Up	p Value (Initial vs. Follow-Up)	p Value (Recurrence vs. Sinus at Follow-UP)
LA dimension, cm	Recurrence	4.72 ± 0.62	4.58 ± 0.64	0.15	0.05
	Sinus	4.31 ± 0.54†	4.16 ± 0.53	0.09	
LAA, cm^2	Recurrence	25.5 ± 8.0	21.9 ± 4.0	0.04	0.01
	Sinus	20.7 ± 3.6†	18.5 ± 3.0	0.01	
LA volume, cm^3	Recurrence	88.1 ± 50.4	66.4 ± 18.4	0.07	0.02
	Sinus	62.3 ± 17.8†	52.4 ± 12.7	0.02	
LA volume index, cm^3/m^2	Recurrence	41.3 ± 22.0	31.2 ± 8.0	0.06	0.007
	Sinus	28.2 ± 7.6†	23.9 ± 6.0	0.02	
Mitral annulus dimension, cm	Recurrence	3.59 ± 0.27	3.48 ± 0.34	0.29	0.06
	Sinus	3.41 ± 0.29	3.24 ± 0.31	0.02	
MRJA, cm^2	Recurrence	7.2 ± 3.0	5.4 ± 3.7	0.11	0.001
	Sinus	5.8 ± 2.5	2.2 ± 1.5	<0.0001	
MRJA/LAA ratio	Recurrence	0.37 ± 0.10	0.28 ± 0.14	0.04	0.005
	Sinus	0.34 ± 0.09	0.16 ± 0.09	<0.0001	
Ejection fraction, %	Recurrence	63 ± 11	62 ± 11	0.73	0.58
	Sinus	61 ± 7	63 ± 5	0.17	
LV end-diastolic dimension, cm	Recurrence	5.10 ± 0.28	5.01 ± 0.32	0.06	0.83
	Sinus	5.06 ± 0.66	5.05 ± 0.53	0.89	
LV end-systolic dimension, cm	Recurrence	3.30 ± 0.41	3.20 ± 0.59	0.52	0.88
	Sinus	3.50 ± 0.65	3.23 ± 0.57	0.02	
Septal thickness, cm	Recurrence	1.22 ± 0.19	1.15 ± 0.17	0.35	0.36
	Sinus	1.14 ± 0.16	1.10 ± 0.13	0.42	
Posterior wall thickness, cm	Recurrence	1.17 ± 0.18	1.11 ± 0.13	0.27	0.36
	Sinus	1.07 ± 0.12	1.06 ± 0.14	0.80	

Values are mean± SD. Echocardiographic characteristics of the patients with significant MR and follow-up echocardiograms are shown. Patients are grouped according to their rhythm status at the time of follow-up echocardiography as recurrence of atrial fibrillation (AF) or sinus rhythm. The p values in the second column from the right represent comparisons between baseline and follow-up within each group. The p values in the final column are for comparisons of follow-up values between the recurrence and sinus rhythm groups. *These numbers are different from 1-year recurrence because status was assessed at time of follow-up echocardiography and only took into account the preceding 6 months. †Baseline comparison between recurrence and sinus groups had significant or near-significant p values for LA dimension (p=0.06), LA area (p=0.02), LA volume (p=0.04), and LA volume index (p=0.02). The remaining baseline comparisons were not significantly different.

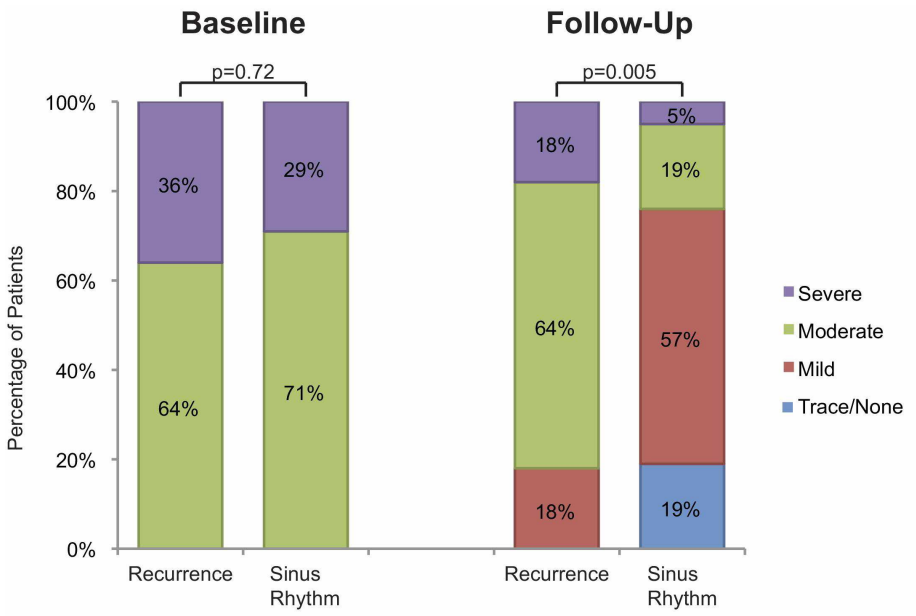

Figure 10.MR Severity at Baseline and Follow-UpPatients are categorized by the rhythm at the time of follow-up as recurrence of atrial fibrillation or sinus rhythm. All patients had moderate or severe mitral regurgitation (MR) at initial echocardiogram. In patients in sinus rhythm at follow-up, only 24% still had moderate or severe MR.

Patients in whom sinus rhythm was maintained after ablation experienced a significant decline in LA size (LA volume index: 27.4 to 23.7 cm^3/m^2, p = 0.02). There was a small, but significant, increase in the degree of MR in the patients with recurrence (MR/LA ratio: 0.09 to 0.11, p = 0.01). In those patients without recurrence, the degree of MR did not change (MR/LA ratio: 0.09 to 0.10, p = 0.62). No patient in the reference cohort developed moderate or worse MR during the follow-up period.

Results 3

Isoproterenol infusion at a dose of 11.05 ± 4.76 μg/min led to induction of sustained AF in 26 patients (93%) that were further studied.

PAF was triggered by APDs from the PVs in 24 patients and from the SVC/RA junction in two. PV triggers were found to originate from the LSPV in 11 (42.3 %), from the LIPV in 2 (7.7 %), from the right PVs in 4 (15.4%). In 7 (26.9%) the trigger was localized to the carina region between LSPV and LIPV.

The arrhythmogenic structures had the highest DF in 22 patients (84.6%) This includes the two patients with RA trigger in whom the highest DF was found in the RA In the remaining patients a slightly higher DF was recorded from non-arrhythmogenic PVs. In the recording there was a significant difference in the DF among the arrhythmogenic structures, the PVs, the LAPW, the CS and the RA (8.07 ± 1.5 Hz vs. 6.65 ± 1.36 Hz vs. 6.06 ± 0.7 Hz vs. 6.01 ± 0.68 Hz vs. 5.93 ± 0.78 Hz, respectively, $p < 0.0001$). The pairwise analysis showed a significantly higher DF in the arrhythmogenic structures compared to the PVs (mean difference 1.42 ± 0.27 Hz, $p < 0.0001$), LAPW (mean difference 2.02 ± 0.32 Hz, $p < 0.0001$), CS (mean difference 2.07 ± 0.32 Hz, $p < 0.0001$), and RA (mean difference 2.15 ± 0.35 Hz, $p < 0.0001$).

Among the 24 patients with PV triggers spontaneous termination occurred in 5 (21%) patients. Acute termination during ablation was observed in 14 (74%) of the remaining 19 patients. Nine of the 14 patients (64%) had AF termination upon isolating the arrhythmogenic PV antrum.(Fig.11) The arrhythmia continued despite arrhythmogenic PV isolation in 10 of 19 patients (53%). Contralateral PV antrum isolation as a second step resulted in AF termination in 5 patients (26%). Another 5 patients were cardioverted

after all PVs were isolated. One of them needed additional lesions for complete PV isolation.

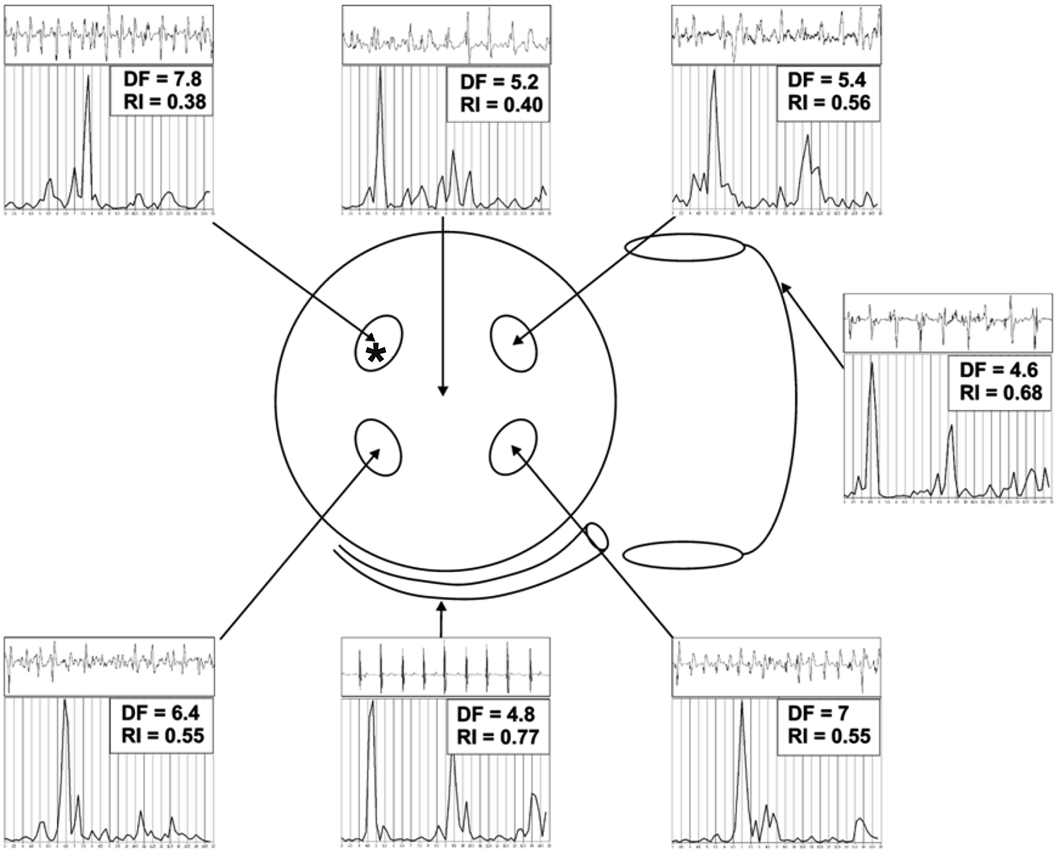

Figure 11. Dominant frequency distribution during AF in one of the patients from the study group in whom the LSPV was found to be the triggering structure as denoted by the asterisk. The arrhythmia terminated upon isolating the left PV antrum. Both atria are presented schematically as if viewed from posterior. The frequency spectrum along with its respective time domain signal is presented for each structure. Numbers represent dominant frequency (DF) and regularity index (RI) for each of the spectra.

Discussion

1. In our study of patients with persistent AF, we found that 1) there is little correlation between the location of CFAE recorded during AF and fractionated

electrograms recorded during sinus rhythm 2) fractionated electrograms recorded during sinus rhythm are mainly caused by wavefront collision in the LA and 3) the presence and distribution of sinus rhythm fractionation in patients with a history of AF is the same as in control patients without a history of AF. Finally, we also found that a signal processing measure, the FFT ratio, closely approximated a manual measure of sinus rhythm fractionation. Together, these findings imply that fractionated electrograms recorded during sinus rhythm, whether measured in the time or frequency domain, are a normal finding in the human LA due to wavefront collision, and are not evidence of underlying tissue characteristics that serve to maintain AF.

It was first noted that patients with persistent AF had more high frequency regions outside the pulmonary veins than patients with paroxysmal AF (9, 36), implying that presence of non-PV AF "drivers" in the left atrial body. These data seemed to be corroborated by Nademanee and colleagues(12), who described termination of persistent AF by targeting high frequency CFAE sites outside the PVs. The mechanism of these CFAEs remains controversial, but may include critical reentry turn-around points, regions of wavefront collision, wavebreak and tissue anisotropy (15, 20, 37, 38). Enthusiasm for the CFAE approach has waned after some investigators were unable to reproduce the initially reported success rates with the CFAE ablation approach (2, 39) However, others have found an improved success rate when CFAE ablation is added to PVI (40) or PVI plus left atrial linear ablation (41).

Rather than identifying abnormal electrograms during AF, Pachon and colleagues (22) identified abnormal electrograms during sinus rhythm, so called "AF Nests." The AF nest approach used a frequency domain measure to identify signals with high frequency content, and found that targeting these regions during sinus rhythm led to an improvement in AF control. It would seem reasonable to hypothesize that there might be a relationship between fractionated electrograms in sinus rhythm (AF nests) and fractionated electrograms recorded during AF (CFAE). Regions that contain fractionated electrograms in sinus rhythm, if activated rapidly and irregularly during AF, might create signals with a high degree of fractionation during AF. This would create a unifying explanation for the improvement in AF control by targeting either AF nests or CFAE, and would provide a target for left atrial substrate modification without requiring the presence

of AF.

However, we found little relationship between CFAE and AF nests. Furthermore, AF nests were primarily due to wavefront collision, with septal predominance likely due to multiple sites of right-to-left atrial breakthrough. Changing the LA activation pattern with CS pacing altered the location of wavefront collision with a parallel shift in the location of AF nests, suggesting that collision was the primary mechanism of SR fractionation. Finally, the presence of a nearly identical distribution of SRF in normal controls with no history of AF suggests that SRF is a normal finding and does not represent a unique pathology supporting AF. The explanation of why AF nest ablation was effective in reducing AF recurrences is unclear, but may be due to autonomic effects or atrial debulking. It is also possible the frequency measure used by Pachon measured some unique property that we were unable to measure; however, our frequency domain measure correlated highly with the time domain measure of fractionation and also showed no relationship to the presence of CFAE.

Several prior studies support our findings that SRF does not represent an abnormal atrial substrate. Roberts-Thompson et al(42) observed fractionated electrograms in the right atrium in a patient population without history of structural heart disease or AF. Similarly, Centurion et al(43) , demonstrated 11-30% fractionated EGMs in the right atrium in a healthy population without a history of AF.

The voltage analysis serves to further support to our hypothesis. We could not demonstrate any significant difference in mean overall LA voltage, or segmental distribution of low voltage areas between the AF and healthy population. This suggests that there was no evidence of left atrial scarring in these patients, and that SRF is therefore a normal finding in healthy control patients. SRF signals were associated with lower voltage amplitudes than non-SRF signals in controls. This may be a consequence of the anisotropic conduction and wavefront collision at these sites, which leads to a cancellation and a reduction of amplitude in these regions in the absence of scar.

2. First , the results of our retrospective cohort study demonstrated , that frequency of mild to moderate or more severe MR is more common in the unique population undergoing AF ablation comparing to historical controls (44). Second ,after a successful

AF ablation procedure, the LA size and dimensions, mitral annular diameters and consequently, the degree of functional MR decreased significantly in a subset of AF patients presented with mild to moderate or more severe MR at baseline in contrast with patients with failed procedure.

We refer to this as atrial functional MR, and clinical characteristics associated with this MR were older age, hypertension, and most powerfully, persistent rather than paroxysmal AF. By echocardiography, MR was associated with increased LA size and mitral annular dilation. After multivariate regression, we found that only age, persistent AF, and mitral annular dilation were linked to MR. This suggests that LA size, notably not independently correlated with MR, may mediate its impact via its effect on the mitral annulus.

By studying follow-up echocardiograms after AF ablation, we were able to evaluate possible pathophysiological mechanisms underlying atrial functional MR. Patients with successful ablations experienced significant reductions in LA size and mitral annular dimension, and less than a third still had significant MR at follow-up. In contrast, among patients who had recurrence of AF, there was no significant change in annular dimension despite near-significant reductions in LA size. Over 80% of the patients with recurrence still had significant MR at follow-up. These findings, combined with those from our regression model, which showed that mitral annular dimension was the only independent echocardiographic predictor of MR, strongly suggest that atrial functional MR is mediated through a process of annular dilatation. Based upon this observation, it can be assumed that beyond the regression of dilated chambers , the potential recovery of the mechanical function can be beneficial on the active motion of mitral leaflets, as Marsan and Tsao et al. demonstrated using four dimensional computed tomographic or real time three dimensional echocardiography (26,28). The precise mechanism by which atrial dysfunction leads to MR merits further exploration. Our findings suggest a crucial role of the mitral annulus, but well-timed atrial contraction is important for appropriate mitral valve closing (45), and the strength and timing of atrial contraction may contribute to normal mitral valve function as well (46).

The prognostic importance of atrial functional MR in the setting of AF is unclear, but potentially significant if one considers parallels in similar disease entities. LA dilatation

itself is an important sign of atrial remodeling, a robust predictor of cardiovascular outcome, and portends worse survival in patients with organic MR (47). Significant ventricular functional MR predicts poorer survival compared with patients with heart failure and normal mitral valve function(48). Worsening severity of organic MR increases mortality risk as well, even in asymptomatic patients (49). However, this may vary depending on the etiology , and long-term studies of the clinical importance of atrial functional MR are warranted.

The most important finding of our study may be that atrial functional MR could potentially be treated without cardiac surgery. Over 80% of patients in the MR cohort had no more than mild residual MR at follow-up with successful restoration of sinus rhythm. Improvement in MR, even without surgery, is not unprecedented in functional MR and medical therapy for heart failure can improve MR severity and functional class The question then is whether all patients with significant atrial functional MR would benefit from a rhythm control approach to treatment of AF.is being unanswered but patients who develop atrial functional MR may represent a subgroup that derives significant clinical benefit from restoration of sinus rhythm. This question would best be answered in a prospective study.

3. This study demonstrates that in most patients with PAF the arrhythmogenic structures show the highest DF peak during spectral analysis. Moreover, termination of PAF by ablation occurs most frequently during isolation of arrhythmogenic PVs. Due to wave breakdown and emergence of complex block pattern multiple, well-demarcated DF domains are formed in the atria - a hallmark of fibrillatory conduction These domains are spatially distributed in a hierarchical order with the highest DF located in the LA and the lowest in the RA.

Studies using frequency mapping during AF in both animal models and humans also support the role of PVs in AF maintenance showing the highest DF to be recorded at the PVs (50).

The presence of a DF gradient from the LA to RA has been shown by Lazar et al. in patients with PAF but not in those with persistent AF (9). This gradient is abolished with

PV isolation and has been found to recover in patients undergoing repeat procedures due to arrhythmia recurrence (10).

Conclusion

1 There is little overlap between regions of CFAE recorded during AF and regions of SR fractionation. During sinus rhythm, fractionated electrograms typically occur in regions of wavefront collision. There is no significant difference in the frequency and distribution of fractionated electrograms recorded during sinus rhythm in patients with and without AF. These findings suggest SRF is not a surrogate for CFAE during AF ablation and SRF itself may not be a suitable ablation target.

2 Patients with AF and significant MR with AF control after RFA had significant reduction in LA dimensions, mitral annular size and MR. These observations suggest a potential relationship between atrial fibrillation and functional mitral regurgitation due to atrial enlargement and annular dilation, and these detrimental effects can be reversed with control of AF after RFA

3 Frequency analysis is a feasible technique which can reliably identify the arrhythmogenic structures which should be the main targets of ablation therapy. in PAF patients

References

1. Haïssaguerre M, Jaïs P, Shah DC, Takahashi A, Hocini M, Quiniou G, Garrigue S, Le Mouroux A, Le Métayer P, Clémenty J. Spontaneous initiation of atrial fibrillation by ectopic beats originating in the pulmonary veins. N Engl J Med. 1998;339(10):659-66.

2. Oral H, Knight BP, Tada H et al. Pulmonary vein isolation for paroxysmal and persistent atrial fibrillation. Circulation. 2002 Mar 5;105(9):1077-81.

3. Moe GK, Abildskov JA. Atrial fibrillation as a self-sustaining arrhythmia independent of focal discharges. Am Heart J 1959;58:59 –70.

4. Allessie MA, Lammers WJEP, Bonke FIM, Hollen SJ. Experimental evaluation of Moe's multiple wavelet hypothesis of atrial fibrillation. In: Zipes DP, Jalife J, eds. Cardiac Electrophysiology and Arrhythmias. NY: Grune & Stratton; 1985:265-275.

5. Mandapati R, Skanes AC, Chen J, Berenfeld O, Jalife J. Stable microreentrant sources as a mechanism of atrial fibrillation in the isolated sheep heart. Circulation. 2000;101:194 –199

6. Berenfeld O, Zaitsev AV, Mironov SF, Pertsov AM, Jalife J.Frequency-dependent breakdown of wave propagation into fibrillatory conduction across the pectinate muscle network in the isolated sheep right atrium. Circ Res. 2002;90(11):1173-80.

7. Harada A, Sasaki K, Fukushima T, Ikeshita M, Asano T, Yamauchi S, Tanaka S, Shoji T. Atrial activation during chronic atrial fibrillation in patients with isolated mitral valve disease.Ann Thorac Surg. 1996; 61(1):104-11.

8. Mansour M, Mandapati R, Berenfeld O, Chen J, Samie FH, Jalife J. Left-to-right gradient of atrial frequencies during acute atrial fibrillation in the isolated sheep heart.

Circulation 2001;103(21):2631-6.

9. Lazar S, Dixit S, Marchlinski FE, Callans DJ, Gerstenfeld EP.Presence of left-to-right atrial frequency gradient in paroxysmal but not persistent atrial fibrillation in humans. Circulation 2004;110(20):3181-6.

10. Lazar S, Dixit S, Callans DJ, Lin D, Marchlinski FE, Gerstenfeld EP. Effect of pulmonary vein isolation on the left-to-right atrial dominant frequency gradient in human atrial fibrillation. Heart Rhythm. 2006; 3(8):889-95.

11. Sanders P, Berenfeld O, Hocini M, Jaïs P, Vaidyanathan R, Hsu LF, Garrigue S, Takahashi Y, Rotter M, Sacher F, Scavée C, Ploutz-Snyder R, Jalife J, Haïssaguerre M. Spectral analysis identifies sites of high-frequency activity maintaining atrial fibrillation in humans. Circulation. 2005;112(6):789-97.

12. Nademanee K, McKenzie J, Kosar E et al. A new approach for catheter ablation of atrial fibrillation: mapping of the electrophysiologic substrate. J Am Coll Cardiol. 2004 Jun 2;43(11):2044-53.

13. Oral H, Chugh A, Yoshida K et al. A randomized assessment of the incremental role of ablation of complex fractionated atrial electrograms after antral pulmonary vein isolation for long-lasting persistent atrial fibrillation. J Am Coll Cardiol. 2009 Mar 3;53(9):782-9.

14. Estner HL, Hessling G, Ndrepepa G et al. Electrogram-guided substrate ablation with or without pulmonary vein isolation in patients with persistent atrial fibrillation. Europace. 2008 Nov;10(11):1281-7

15. Konings KT, Kirchhof CJ, Smeets JR, Wellens HJ, Penn OC, Allessie MA. High-density mapping of electrically induced atrial fibrillation in humans. Circulation. 1994 Apr;89(4):1665-80

16: Zlochiver S, Yamazaki M, Kalifa J, Berenfeld O. Rotor meandering contributes to irregularity in electrograms during atrial fibrillation. Heart Rhythm. 2008 Jun;5(6):846-54.

17. Jacquemet V, Henriquez CS. Genesis of complex fractionated atrial electrograms in zones of slow conduction: a computer model of microfibrosis. Heart Rhythm 2009 Jun;6(6):803-10.

18. Park JH, Pak HN, Kim SK et al. Electrophysiologic characteristics of complex fractionated atrial electrograms in patients with atrial fibrillation. J Cardiovasc Electrophysiol. 2009 Mar;20(3):266-72.

19. Stiles MK, Brooks AG, Kuklik P et al. High-density mapping of atrial fibrillation in humans: relationship between high-frequency activation and electrogram fractionation. J Cardiovasc Electrophysiol. 2008 Dec;19(12):1245-53.

20. Rostock T, Rotter M, Sanders P et al. High-density activation mapping of fractionated electrograms in the atria of patients with paroxysmal atrial fibrillation. Heart Rhythm. 2006 Jan;3(1):27-34.

21. Stiles MK, John B, Wong CX et al. Paroxysmal lone atrial fibrillation is associated with an abnormal atrial substrate: characterizing the "second factor". J Am Coll Cardiol. 2009 Apr 7;53(14):1182-91.

22. Pachon M JC, Pachon M EI, Pachon M JC et al. A new treatment for atrial fibrillation based on spectral analysis to guide the catheter RF-ablation. Europace. 2004 Nov;6(6):590-601.

23. Arruda M, Natale A. Ablation of permanent AF: adjunctive strategies to pulmonary veins isolation: targeting AF NEST in sinus rhythm and CFAE in AF. J Interv Card Electrophysiol. 2008 Oct;23(1):51-7.

24. Schoonderwoerd BA, Van Gelder IC, Van Veldhuisen DJ, Van den Berg MP, CrijnsHJ. Electrical and structural remodeling: role in the genesis and maintenance of atrial fibrillation. Prog Cardiovasc Dis. 2005 Nov-Dec;48(3):153-68.

25. Dittrich HC, Pearce LA, Asinger RW, McBride R, Webel R, Zabalgoitia M, Pennock GD, Safford RE, Rothbart RM, Halperin JL, Hart RG. Left atrial diameter in nonvalvular atrial fibrillation: An echocardiographic study. Stroke Prevention in Atrial Fibrillation Investigators. Am Heart J. 1999 Mar;137(3):494-9.

26. Marsan NA, Tops LF, Holman ER, Van de Veire NR, Zeppenfeld K, Boersma E, van der Wall EE, Schalij MJ, Bax JJ. Comparison of left atrial volumes and function by real-time three-dimensional echocardiography in patients having catheter ablation for atrial fibrillation with persistence of sinus rhythm versus recurrent atrial fibrillation three months later. Am J Cardiol. 2008 Oct 1;102(7):847-53.

27. Reant P, Lafitte S, Jaïs P, Serri K, Weerasooriya R, Hocini M, Pillois X, Clementy J, Haïssaguerre M, Roudaut R. Reverse remodeling of the left cardiac chambers after catheter ablation after 1 year in a series of patients with isolated atrial fibrillation. Circulation. 2005 Nov 8;112(19):2896-903.

28. Tsao HM, Hu WC, Wu MH, Tai CT, Chang SL, Lin YJ, Lo LW, Huang CC, Hu YF, Sheu MH, Chang CY, Chen SA. The Impact of Catheter Ablation on the Dynamic Function of the Left Atrium in Patients with Atrial Fibrillation: Insights from Four-Dimensional Computed Tomographic Images. J Cardiovasc Electrophysiol. 2009 Oct 5.

29. Sanfilippo AJ, Abascal VM, Sheehan M, Oertel LB, Harrigan P, Hughes RA, Weyman AE. Atrial enlargement as a consequence of atrial fibrillation. A prospective echocardiographic study. Circulation. 1990 Sep;82(3):792-7.

30. Perloff JK, Roberts WC. The mitral apparatus. Functional anatomy of mitral regurgitation. Circulation. 1972 Aug;46(2):227-39. PubMed PMID: 5046018.

31. Otsuji Y, Kumanohoso T, Yoshifuku S, Matsukida K, Koriyama C, Kisanuki A, Minagoe S, Levine RA, Tei C. Isolated annular dilation does not usually cause important functional mitral regurgitation: comparison between patients with lone atrial fibrillation and those with idiopathic or ischemic cardiomyopathy. J Am Coll Cardiol. 2002 May 15;39(10):1651-6.

32: Tanimoto M, Pai RG. Effect of isolated left atrial enlargement on mitral annular size and valve competence. Am J Cardiol. 1996 Apr 1;77(9):769-74.

33. Park SM, Park SW, Casaclang-Verzosa G, Ommen SR, Pellikka PA, Miller FA Jr, Sarano ME, Kubo SH, Oh JK. Diastolic dysfunction and left atrial enlargement as contributing factors to functional mitral regurgitation in dilated cardiomyopathy: data from the Acorn trial. Am Heart J. 2009 Apr;157(4):762.e3-10.

34. de Bakker JM, Wittkampf FH. The pathophysiologic basis of fractionated and complex electrograms and the impact of recording techniques on their detection and interpretation. Circ Arrhythm Electrophysiol. 2010 Apr 1;3(2):204-13.

35. Calkins H, Brugada J, Packer DL, et al. HRS/EHRA/ECAS expert consensus statement on catheter and surgical ablation of atrial fibrillation: recommendations for personnel, policy, procedures and followup: a report of the Heart Rhythm Society (HRS) Task Force on Catheter and Surgical Ablation of Atrial Fibrillation. Europace 2007; 9:335–79.

36. Haïssaguerre M, Sanders P, Hocini M et al. Catheter ablation of long-lasting persistent atrial fibrillation: critical structures for termination. J Cardiovasc Electrophysiol. 2005 Nov;16(11):1125-37.

37. Cosio FG, Palacios J, Vidal JM, Cocina EG, Gómez-Sánchez MA, Tamargo L. Electrophysiologic studies in atrial fibrillation. Slow conduction of premature impulses: a possible manifestation of the background for reentry. Am J Cardiol.

1983 Jan 1;51(1):122-30.

38. Spach MS, Dolber PC. Relating extracellular potentials and their derivatives to anisotropic propagation at a microscopic level in human cardiac muscle. Evidence for electrical uncoupling of side-to-side fiber connections with increasing age. Circ Res. 1986 Mar;58(3):356-71

39. Deisenhofer I, Estner H, Reents T et al. Does electrogram guided substrate ablation add to the success of pulmonary vein isolation in patients with paroxysmal atrial fibrillation? A prospective, randomized study. J Cardiovasc Electrophysiol. 2009 May;20(5):514-21.

40. Elayi CS, Verma A, Di Biase L et al .Ablation for longstanding permanent atrial fibrillation: results from a randomized study comparing three different strategies. Heart Rhythm. 2008 Dec;5(12):1658-64.

41. Lin YJ, Tai CT, Chang SL et al. Efficacy of additional ablation of complex fractionated atrial electrograms for catheter ablation of nonparoxysmal atrial fibrillation. J Cardiovasc Electrophysiol. 2009 Jun;20(6):607-15.

42. Roberts-Thomson KC, Kistler PM, Sanders P et al. Fractionated atrial electrograms during sinus rhythm: relationship to age, voltage, and conduction velocity. Heart Rhythm. 2009 May;6(5):587-91.

43. Centurión OA, Shimizu A, Isomoto S, et al. Influence of advancing age on fractionated right atrial endocardial electrograms. Am J Cardiol. 2005 Jul 15;96(2):239-42.

44. Singh JP, Evans JC, Levy D, Larson MG, Freed LA, Fuller DL, Lehman B, Benjamin EJ. Prevalence and clinical determinants of mitral, tricuspid, and aortic regurgitation (the Framingham Heart Study). Am J Cardiol. 1999 Mar15;83(6):897-902. Erratum in: Am J

Cardiol 1999 Nov 1;84(9):1143

45. David D, Michelson EL, Naito M, Chen CC, Schaffenburg M, Dreifus LS. Diastolic "locking" of the mitral valve: the importance of atrial systole and intraventricular volume. Circulation 1983;67:640 –5.

46. Dell'Era G, Rondano E, Franchi E, Marino PN. Atrial asynchrony and function before and after electrical cardioversion for persistent atrial fibrillation. Eur J Echocardiogr 2010;11:577– 83.

47.Le Tourneau T, Messika-Zeitoun D, Russo A, et al. Impact of left atrial volume on clinical outcome in organic mitral regurgitation. J Am Coll Cardiol 2010;56:570–8.

48. Trichon BH, Felker GM, Shaw LK, Cabell CH, O'Connor CM. Relation of frequency and severity of mitral regurgitation to survival among patients with left ventricular systolic dysfunction and heart failure. Am J Cardiol 2003;91:538–43.

49. Enriquez-Sarano M, Aviernos J-F, Messika-Zeitoun D, et al. Quantitative determinants of the outcome of asymptomatic mitral regurgitation. N Eng J Med 2005;352:875– 83.

50. Sanders P, Berenfeld O, Hocini M, et al: Spectral analysis identifies sites of high-frequency activity maintaining atrial fibrillation in humans. Circulation. 2005;112(6):789-97.

Acknowledgements

First of all, I would like to express my gratitude to Prof. Dr. Csanády Miklós the former head of the Second Department of Medicine and Cardiology Center, who gave me the chance to work at the institution and to my supervisor Prof. Dr. Forster Tamás for his continous support and guidance.

I'm especially grateful to David J. Callans, Edward P. Gerstenfeld, and Francis E. Machlinski from the Hospital of University of Pennsylvania, Philadelphia, USA for the research ideas , the common work and support of cooperation between our groups.

Many thanks to the Cardiac Electrophysiolgy Team of the Cardiology Center for their contribution and excellent work. Especially thank to my closest colleague Robert Pap, for his personal help and outstanding ideas.

I dedicate this Thesis to my Wife, Anita and my Children, László, Álmos and Szabolcs for their unbelievable patience, support and love.

Összefoglalás

Bevezetés

A pitvarfibrilláció a leggyakoribb szupraventrikuláris ritmuszavar. A tüdő- és egyes mellkasi vénák szerepe mind a ritmuszavar elinditásában mind pedig fenntartásában bizonyított. Ennek megfelelően a pulmonális véna izoláció vált a paroxysmális pitvarfibrilláció legsikeresebb kezelési stratégiájává, azonban a perzisztens pitvarfibrillácó intervenciós kezelésében ez többnyire nem elégséges hanem egyéb kiegészítő, elsősorban a bal pitvari szubsztrát modifikációját szolgáló módszerek lehetnek szükségesek. Ennek keretében mind a pitvarfibrilláció alatt regisztrált komplex frakcionált elektrogrammok által jellemzett mind pedig a sinus ritmusban felvett fragmentált szignált eredményező pitvari régiók lehetnek az ablációs kezelés célpontjai. A két típusú fragmentáció között azonban az összefüggés nem ismert.

A legelterjedtebb módszer a pitvari elektromos aktiváció jellemzésére a pitvari ciklushossz mérése a megszokott time domain módszerrel, azonban a fent említett frakcionáció ezt nagymértékben nehezíti. Emiatt egyéb módszerek válnak egyre elterjedtebbé melyek a pitvari elektrogrammok spektrális jellemzésére építenek és ezáltal pontosabb analízist tesznek lehetővé ezen fragmentált elektrogrammok térbeli különbözőségének viszgálatára.

A pitvarfibrilláció egyedi elektromos megjelenésén túl szintén fontossággal bír a ritmuszavar bal pitvari remodellinget okozó hatása. Ezen átalakulás potenciális hatása a mitrális billentyűfunkcióra és esetleges etiológiai szerepe a funkcionális mitrális regurgitáció létrehozásában kevéssé ismert.

Célkitűzések

1. A pitvarfibrilláció alatt észlelt komplex fragmentált elektrogrammokat mutató és a sinus ritmusban hasonló szignáltulajdonságokkal jellemzett bal pitvari területek eloszlásának illetve feltételezett kapcsolatának vizsgálata, valamint a sinus ritmus fragmentáció mechanizmusának tisztázása.

2. Azon feltevés igazolása hogy pitvarfibrillációban és szignifikáns mértékű mitrális billentyűelégtelenségban szenvedő betegekben a sikeres radiófrekvenciás ablációt

követően reverz bal pitvari remodelling és ezzel összefüggésben javuló mitrális billentyűfunkció észlelhető.

3. A bal pitvar valamint a pulmonális véna elektrogrammok spectrális analízise, ezen belül a domináns frekvenciák térbeli eloszlásának, valamint az ezen módszerrel aritmogénnek bizonyult tüdővénák rádiófrekvenciás ablációra adott válaszának vizsgálata.

Módszerek

1.. Bal pitvari elektroanatómiai térkép készült 20 perzisztensen pitvarfibrilláló betegben(62±9 év, 13 férfi) valamint kontroll populációként 9, struktúrális szívbetegségben nem de egyéb aritmia miatt vizsgált betegben(36±6 év, 4 férfi). A pitvarfibrilláció alatt CFAE elektrogrammok által jellemzett és ugyanabban a betegben sinus ritmusban fragmentált területek közötti kapcsolat került vizsgálatra valamint utóbbi területek kapcsolata került elemzésre összehasonlítva az aktivációs térképeken észlelt propagációs mintákkal valamint a kontroll populációval.

2. Retrospektív analízis során 828 pitvarfibrilláció abláción átesett beteg adatai kerültek elemzésre melynek során 53 olyan beteg került regisztrálásra , akiben legalább közepes fokú mitrális regurgitáció volt felfedezhető. Ennek megfelelően ugyancsak 53 beteg került kontroll csoportként kiválasztásra abból a kohortból ahol a mitrális elégtelenség foka közepesnél kisebbnek bizonyult. Ezen csoportokban a perioperatív és az utánkövetés klinikai és echocardiográphiás adatai kerültek összehasonlításra az ablációs siker függvényében.

3. Pitvarfibrilláció indukció történt isoproterenol adagolásával 26 paroxysmálisan pitvarfibrilláló betegben (15férfi, 55 ±8.4 év) rádiófrekvenciás abláció során. Ezek után a tartós pitvarfibrillációs epizód alatt multipoláris diagnosztikus katéter segítségével intracardiális jelrögzítés történt a bal pitvarban a pulmonális vénák, a hátsó fal, a sinus coronarius és a jobb pitvar meghatározott területeiről. Minden említett területről Fast – Fourier transzformáció segítségével a domináns frekvencia került meghatározásra, és ennek eloszlása valamint az ez alapján aritmogénnek tartott pulmonális véna izoláció kapcsán bekövetkezett változások kerültek vizsgálatra.

Eredmények

1. SRF (338±150 térképpont) és a CFAE (418±135 térképpont) 29±14 és 25±15 %-át foglalták el a teljes bal pitvari felszínnek külön-külön A térképeken szignifikáns összefüggés a SRF és CFAE régiók elhelyezkedésében nem volt kimutatható(r=0.2, P=NS). A pitvarfibrilláló és kontroll betegek közötti összehasonlításban azonban a SRF-t mutató területek eloszlása megegyezett(p=0.74). A SRF-t mutató területek az esetek 75 %-ban a hullámfront –találkozási régiókban helyezkedtek el az aktivációs térképeken.

2. A szignifikáns mértékű mitrális regurgitációt mutató betegek idősebbek voltak és gyakrabban szenvedtek a ritmuszavar perzisztens formájában (62% vs. 23%, p <0.0001). Ugyancsak ezen betegek esetében nagyobb bal pitvari dimenziók és mitrális annuláris méretek voltak detektálhatók (volume index: 32 cm3/m2 vs. 26 cm3/m2, p =0.008 és 3.49 cm vs. 3.23 cm, p = 0.001), de bal kamrai dimenzióik nem különböztek a kontroll csoporttól. A mitrális annulus mérete, az életkor valamint a pitvarfibrilláció perzisztens volta bizonyult a szignifikáns mértékű mitrális regurgitáció független prediktorának. Az utánkövetés echokardiographiás adatai alapján a sinus ritmus tartós fennmaradása esetén nagyobb mértékű bal pitvari és mitrális annuláris méretcsökkenés, és a szignifikáns mértékű mitrális regurgitáció arányának csökkenése (24% vs. 82%, p= 0.005) volt igazolható azon betegekhez képest ahol a sinus ritmus tartósan nem maradt fenn azaz a beavatkozás hosszabb távon sikertelennek bizonyult.

3. A paroxysmalis pitvarfibrillációs epizódok 24 betegben a tüdővénákból két betegben pedig a jobb pitvarból eredtek. Szignifikáns mértékű frekvenciagrádiens volt kimutatható a domináns frekvenciák vonatkozásában az aritmogén struktúrák felől az egyéb pulmonális vénák, sinus coronarius, hátsó fal és jobb pitvar felé (p < 0.0001). A betegek 64 %-ában a pitvarfibrilláció a DF analízis alapján aritmogénnek tartott pulmonális véna izolációja kapcsán szűnt meg.

Következtetések

Lényeges összefüggés nem mutatható ki a CFAE-t és a SRF-t mutató bal pitvari regiók vonatkozásában függetlenül attól hogy time- vagy frekvencia domain módszerekkel került-e a fragmentáció foka meghatározásra. A SRF leginkább az aktivációs hullámfront-találkozással áll öszefüggésben és ezen régiók eloszlása lényegesen nem különbözött az egészséges kontroll csoportban észleltektől. Ezen megfigyelések alapján megállapítható hogy a perzisztens pitvarfibrilláció mechanizmusában a sinus ritmusban észlelhető fragmentált régiók nem játszanak lényegi szerepet és ablációs célpontként kevéssé jönnek szóba.

A szignifikáns funkcionális mitrális regurgitációban szenvedő pitvarfibrilláló betegekben a sikeres ablációt követően a bal pitvari és mitrális annuláris méretek, valamint a mitrális regurgitáció foka csökkent. Ez a megfigyelés felhívja a figyelmet a pitvarfibrilláció okozta bal pitvari remodelling mitrális apparátusra gyakorolt káros hatására, mely azonban visszafordítható a sikeres beavatkozást követő tartós sinus ritmus mellett.

A paroxysmálisan pitvarfibrilláló betegekben a triggerelő struktúra mutatta a leggyorsabb aktivitást spektrális analízis során, ennek megfelelően itt volt a legmagasabb DF regisztrálható.